



## A Significant Approach in which a Carboxylic Acid Group Prevents Bisindole Formation when 2-Formylbenzoic Acid Reacts with Indole: A Crystal Structure Study

R. Anil Kumar<sup>1</sup>, S. Naveen<sup>2</sup>, M. N. Kumara<sup>3</sup>,  
K. M. Mahadevan<sup>4</sup> and N. K.Lokanath<sup>5\*</sup>

<sup>1,4</sup>Department of Chemistry, Kuvempu University, P. G. Centre, Kadur 577548, India.

<sup>2</sup>Institution of Excellence, VijnanaBhavana, Manasagangotri, University of Mysore, Mysuru 570006, India.

<sup>3</sup>Department of Chemistry, Yuvaraja's College, University of Mysore, Mysuru 570 006, India

<sup>4</sup>Department of Studies in Physics, Manasagangotri, University of Mysore, Mysuru 570006, India.

**Abstract :** Expedite, highly efficient and a novel procedure for the synthesis of 3-(1*H*-indol-3-yl)-2-benzofuran-1(3*H*)-ones *via* condensation reaction of indole and 2-formylbenzoic acid catalyzed by glacial acetic acid with excellent yield have been described. The products obtained were characterized by IR, <sup>1</sup>H NMR, LCMS spectral analysis and finally the structure was confirmed by single crystal X-ray diffraction studies. The compound The C<sub>16</sub>H<sub>10</sub>FNO<sub>2</sub> crystallizes in the orthorhombic space group Pbc<sub>a</sub> with a single molecule in the asymmetric unit. The crystal structure revealed the presence of intermolecular hydrogen bonds of the type N—H...O and C—H...O which contributes to the crystal packing. Further, Hirshfeld surface studies revealed the nature of intermolecular contacts; the importance of the molecular interactions are established from  $d_{norm}$ , electrostatic potential and fingerprint plot, which provides the information about the percentage contribution of the individual intermolecular contacts to the surface.

**Key Words :** Bis-Indoles; 3-(1*H*-indol-3-yl)-2-benzofuran-1(3*H*)-ones; Crystal Structure; Hirshfeld surface analysis, Fingerprint plots.

### Introduction

Indoles are found to be one of the significant groups of compounds used for various physiological and biological activities [1-3]. On the other hand, various bis(indolyl)methanes have also attracted considerable attention due to their potential biological activities [4-7]. Hence while attempting to obtain such lead bioactive bisindolylmethanes we unexpectedly ended with a strange product when we carried out a reaction between 2-formylbenzoic acid and indole in the presence of glacial acetic acid at room temperature stirring for 4-6 hours (**Scheme-1**). Initially one molecule of 2-formylbenzoic acid and two molecules of indole reaction were carried out. But the products obtained was 3-(1*H*-indol-3-yl)-2-benzofuran-1(3*H*)-ones (**4a-b**). Then we realized that the reaction occurred by utilizing mole equivalents of 2-formylbenzoic acid and indole (1:1). Further the same reaction was repeated with mole equivalent of 2-formylbenzoic acid and indole (**Scheme-2**) to furnish the new products **4a** and **4b**. In view of the wide applications associated with the Indole derivatives and in continuation

of our work on new products isolation and their single crystal structure studies [8-11], we report herein an interesting reaction and its end products 3-(1*H*-indol-3-yl)-2-benzofuran-1(3*H*)-ones (**4a-b**). The product obtained was characterized spectroscopically by NMR and IR techniques and finally the structure was confirmed X-ray diffraction studies.

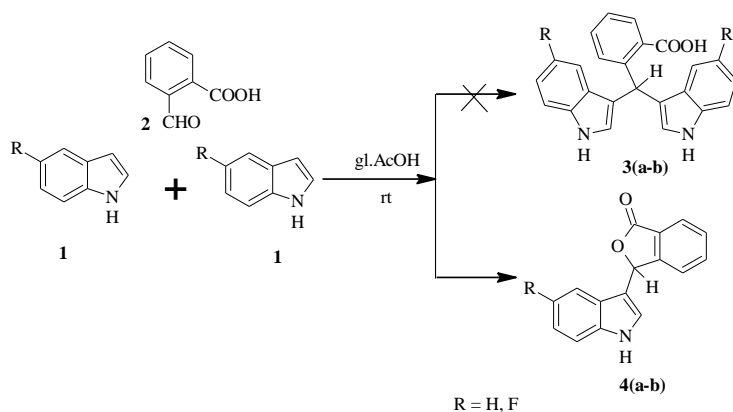
## Experimental Procedure

### Materials and methods

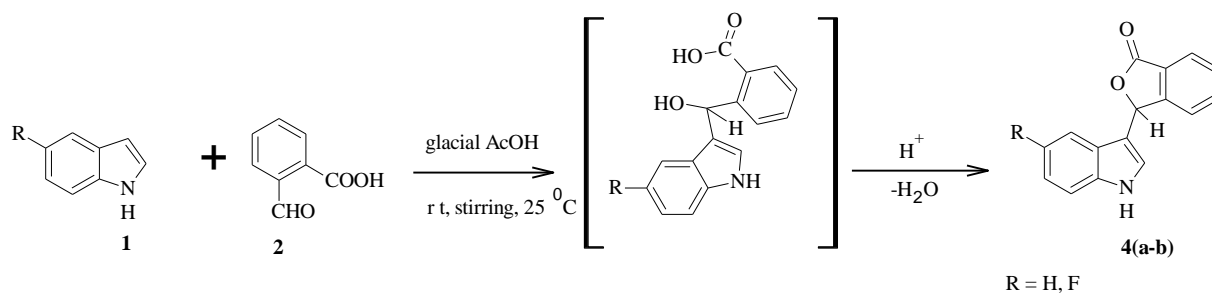
In a flask containing 5 ml of glacial acetic acid and indole (1 mmol, 0.50 g) was added under stirring until all the indole was dissolved. Then 2-formylbenzoic acid (1 mmol, 0.64 g) was added under vigorous stirring. The reaction mixture was allowed to stir for 4-6 h, where the reaction solution turned from light yellow to light pink to dark red color. The product formation was detected by TLC (100 % CH<sub>2</sub>Cl<sub>2</sub>). After the completion of the reaction, the reaction mixture was added to the ice cold water. The product separated out from the reaction mixture was filtered and washed with water. The crude product was further purified by recrystallization by using methanol furnished white crystals of 3-(1*H*-indol-3-yl)-2-benzofuran-1(3*H*)-one (**4a**) in good yield (80.5%), M.P = 174-176<sup>0</sup>C. Similarly, the compound 3-(5-fluoro-1*H*-indol-3-yl)-2-benzofuran-1(3*H*)-one (**4b**) was also synthesized, purified and recrystallized. (Yield, 83%, and M.P=180-182<sup>0</sup>C).

### Synthesis of 3-(1*H*-indol-3-yl)-2-benzofuran-1(3*H*)-ones

The reaction sequence used for synthesis of 3-(1*H*-indol-3-yl)-2-benzofuran-1(3*H*)-one (**4a**) is depicted in **Scheme-1**. The 3-(1*H*-indol-3-yl)-2-benzofuran-1(3*H*)-one (**4a**) was accomplished by condensation reaction by using commercially available indole (**1**) and 2-formylbenzoic acid (**2**). Stirring the reaction mixture with glacial acetic acid at RT for 4-6 h gave unexpected cyclisation product called 3-(1*H*-indol-3-yl)-2-benzofuran-1(3*H*)-one (**4a**) instead of corresponding bis(indolyl)methane (**3a**). Thus the resulted crude product was purified by recrystallization using methanol as solvent to get 3-(1*H*-indol-3-yl)-2-benzofuran-1(3*H*)-one (**4a**). Recrystallization with methanol resulted fine white crystals of 3-(1*H*-indol-3-yl)-2-benzofuran-1(3*H*)-one (**4a**). The product structure was established by single crystal X-ray diffraction studies.

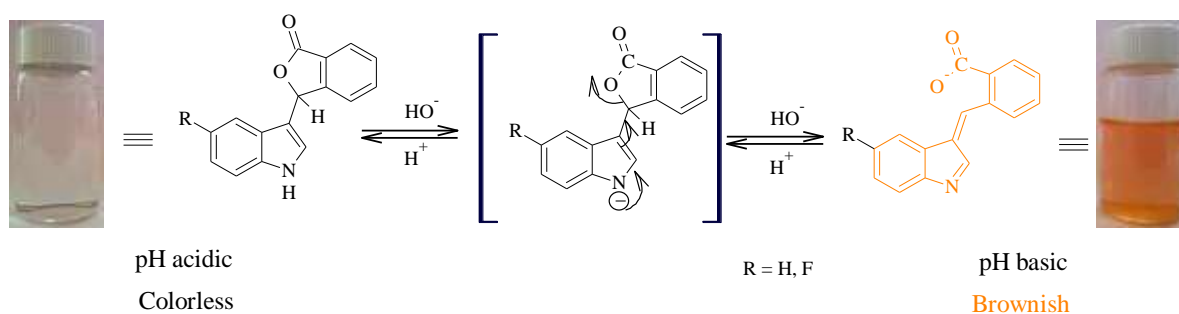


**Scheme-1: Reaction of indole (1) and 2-formylbenzoic acid (2) to obtain unexpected 3-(1*H*-indol-3-yl)-2-benzofuran-1(3*H*)-ones (4a-b)**



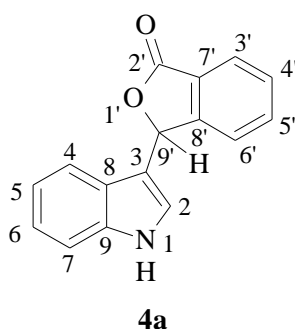
**Scheme-2: Mole equivalent reaction of indole (1) and 2-formylbenzoic acid (2) to obtain 3-(1*H*-indol-3-yl)-2-benzofuran-1(3*H*)-ones (4a-b)**

Similarly, the compound 3-(5-fluoro-1*H*-indol-3-yl)-2-benzofuran-1(3*H*)-one (4b) was also obtained under the same reaction conditions. Hence, we proved that any structure of appropriate indoles can produce similar products. Since, the structure resembles with the structure of phenolphthalein in its chemical properties, the following reaction with NaOH was checked for compound 4a and their color change was examined as shown in Scheme-3. Thus we concluded that these compounds can also be very useful in similar application in which phenolphthalein's are being used for biochemical or physico chemical applications.



**Scheme-3: Physical changes of 3-(1*H*-indol-3-yl)-2-benzofuran-1(3*H*)-one (4a) in both acidic and basic pH**

The postulated structure of the newly synthesized 3-(1*H*-indol-3-yl)-2-benzofuran-1(3*H*)-one compound 4a was in good agreement with structure based on their IR, <sup>1</sup>H NMR, and X-ray diffraction studies.



### X-ray Diffraction Studies

A white colored rectangle shaped single crystal of dimensions 0.29×0.26×0.22 mm of the title compound was chosen for an X-ray diffraction study. The X-ray intensity data were collected at a temperature of 296 K on a Bruker Proteum2 CCD diffractometer equipped with an X-ray generator operating at 45 kV and 10 mA, using CuK<sub>α</sub> radiation of wavelength 1.54178 Å. Data were collected for 24 frames per set with different settings of φ(0° and 90°), keeping the scan width of 0.5°, exposure time of 2 s, the sample to detector distance of 45.10 mm and 2θ value at 46.6°. A complete data set was processed using *SAINT PLUS* [12]. The structure was solved by direct methods and refined by full-matrix least squares method on *F*<sup>2</sup> using *SHELXS* and

*SHELXL* programs [13]. All the non-hydrogen atoms were revealed in the first difference Fourier map itself. All the hydrogen atoms were positioned geometrically and refined using a riding model with  $U_{\text{iso}}(\text{H}) = 1.2 U_{\text{eq}}$  and  $1.5 U_{\text{eq}}(\text{O})$ . After ten cycles of refinement, the final difference Fourier map showed peaks of no chemical significance and the residuals saturated to 0.0343. The geometrical calculations were carried out using the program *PLATON* [14]. The molecular and packing diagrams were generated using the software *MERCURY* [15].

### Hirshfeld surface calculations

Hirshfeld surface analysis was carried out and finger print plots were plotted using the software Crystal Explorer 3.0 [16]. The  $d_{\text{norm}}$  plots were mapped with color scale in between  $-0.18$  au (blue) and  $1.4$  au (red). The 2D fingerprint plots [17, 18] were displayed by using the expanded  $0.6\text{--}2.8$  Å view with the  $d_e$  and  $d_i$  distance scales displayed on the graph axes. When the cif file was uploaded into the Crystal Explorer software, all bond lengths to hydrogen were automatically modified to typical standard neutron values i.e.,  $\text{C-H} = 1.083$  Å.

### Results and discussion

The compound **4a** exhibited IR absorption band at  $3311\text{ cm}^{-1}$  due to indole -NH group, band at  $3055\text{ cm}^{-1}$  indicates -CH- stretching, another characteristic absorption band at  $1732\text{ cm}^{-1}$  which is slightly higher stretching frequency ( $\text{C=O}$ ) strongly suggest the presence of cyclic ester group in compound **4a** (Figure 2).

The  $^1\text{H}$  NMR spectra (Figure 1(a) and 1(b)) of the compound 3-(1*H*-indol-3-yl)-2-benzofuran-1(3*H*)-one (**4a**) showed the 10 aromatic protons between 6.76-8.36 ppm. In this, one sharp singlet at  $\delta=6.96$  signifies the presence of tertiary proton which is located at the junction of the indole ring and benzo-2-furanone rings linked together. Further a broad singlet of indole -NH appears at 11.31 ppm, and remaining aromatic protons appears as triplet at  $\delta=6.87$  ppm with coupling constant,  $J=7.00$  Hz, another in the range of 7.08 ppm with coupling constant,  $J=7.60$  Hz, at 7.40 ppm with coupling constant,  $J=8.40$  Hz, the four doublet, one in the  $\delta=6.78$  ppm with coupling constant,  $J=8.00$  Hz, at 7.40 ppm with coupling constant  $J=8.40$  Hz, at 7.95 ppm with coupling constant,  $J=7.60$  Hz respectively are in consistence with the depicted structure.

Thus from all these spectral evidence and single crystal structural analysis the structure of compound **4a** was confirmed.

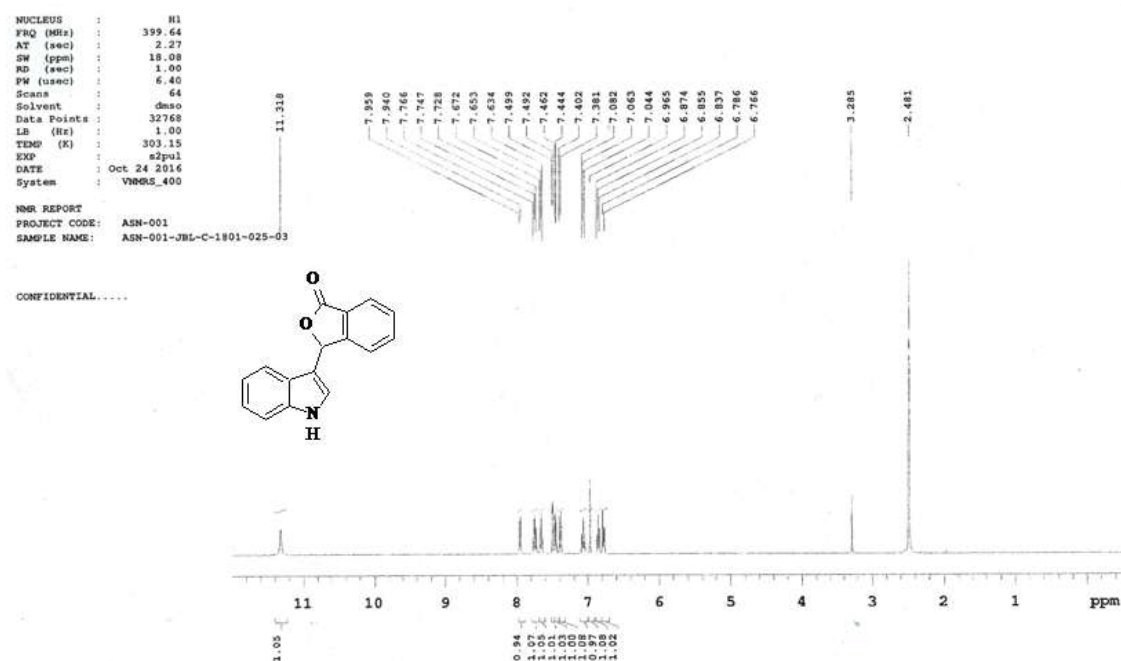


Figure 1(a):  $^1\text{H}$  NMR Spectrum of 3-(1*H*-indol-3-yl)-2-benzofuran-1(3*H*)-one (**4a**)

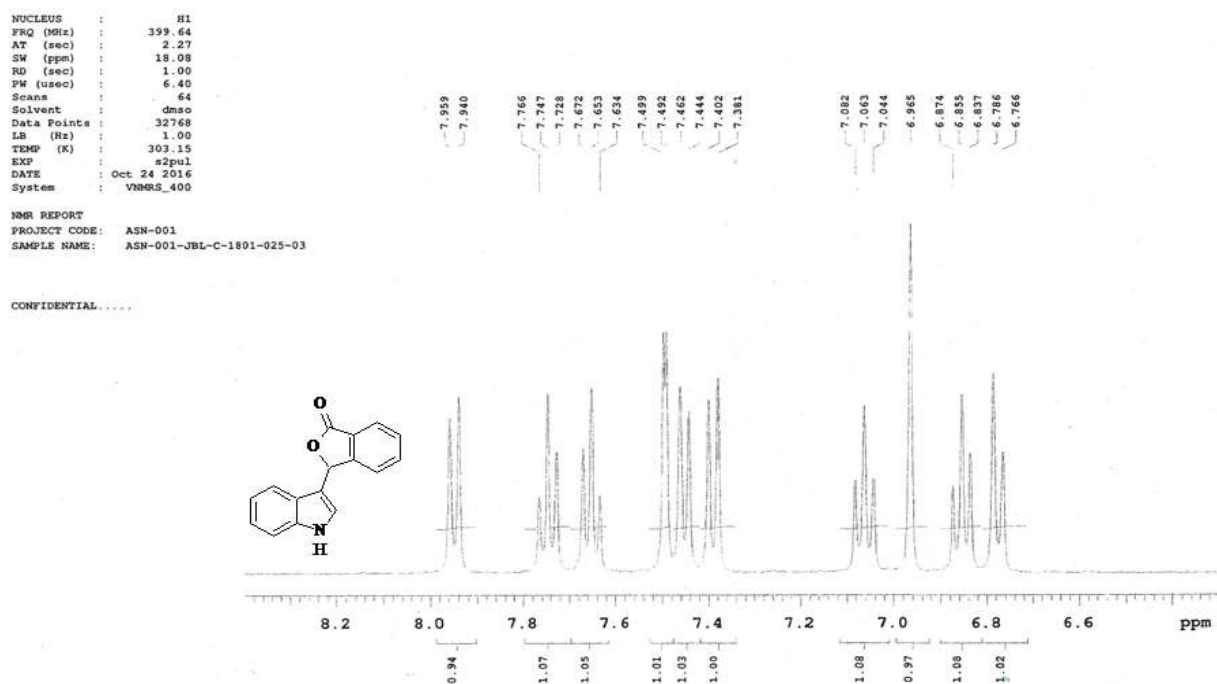
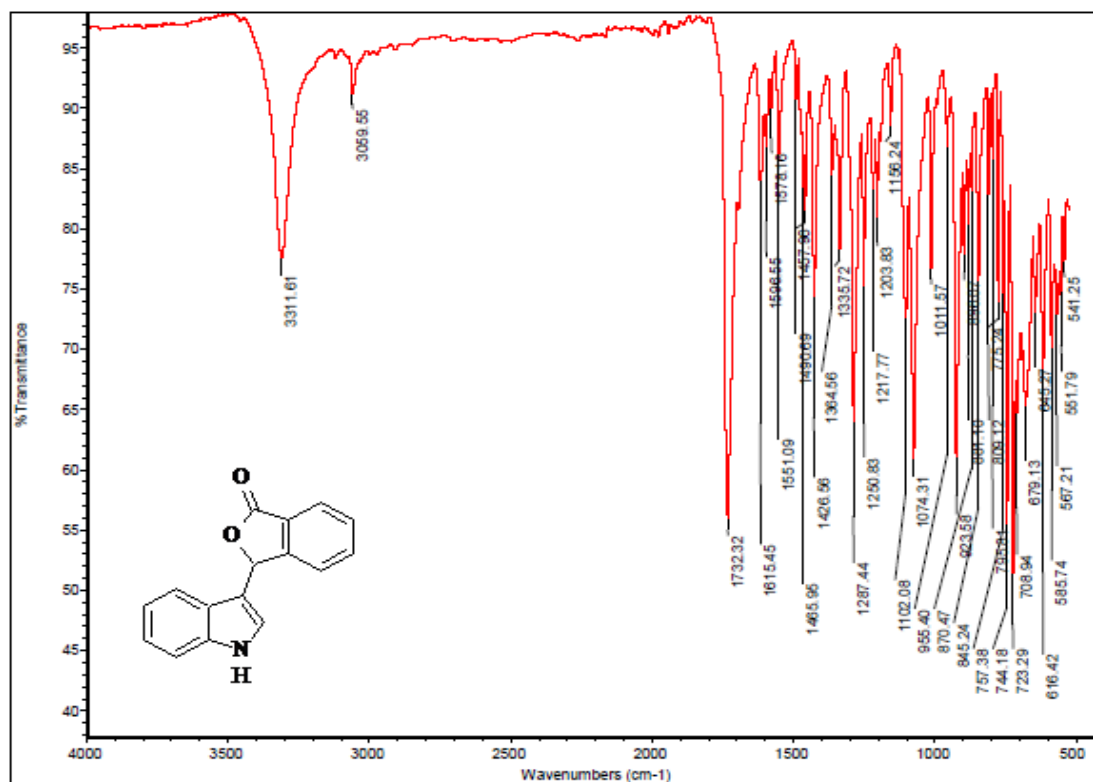
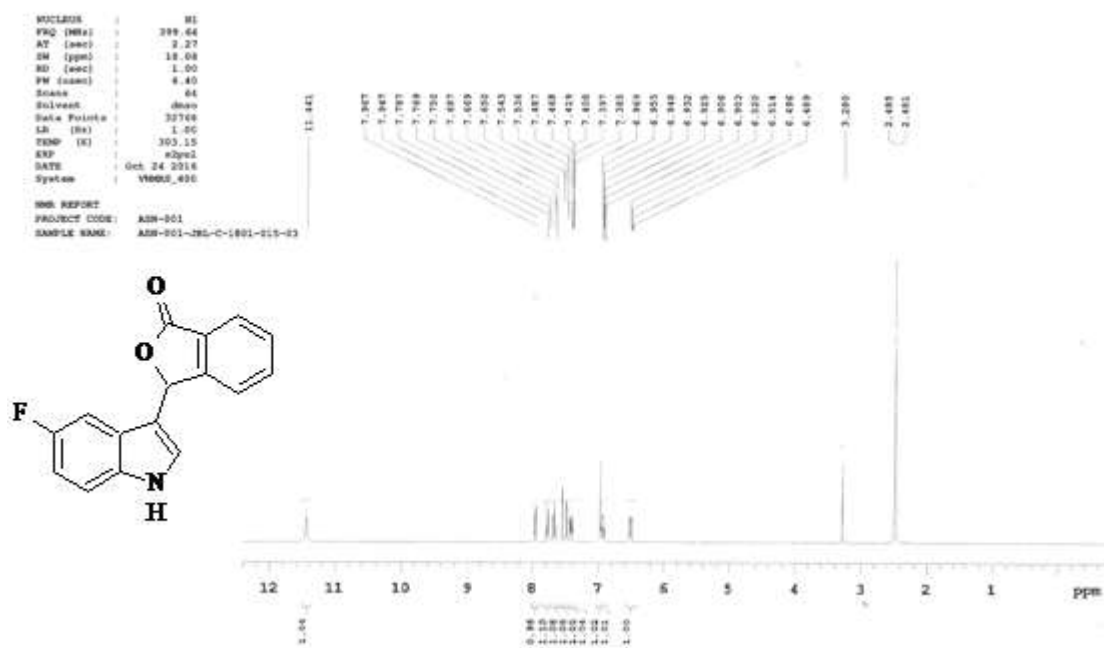
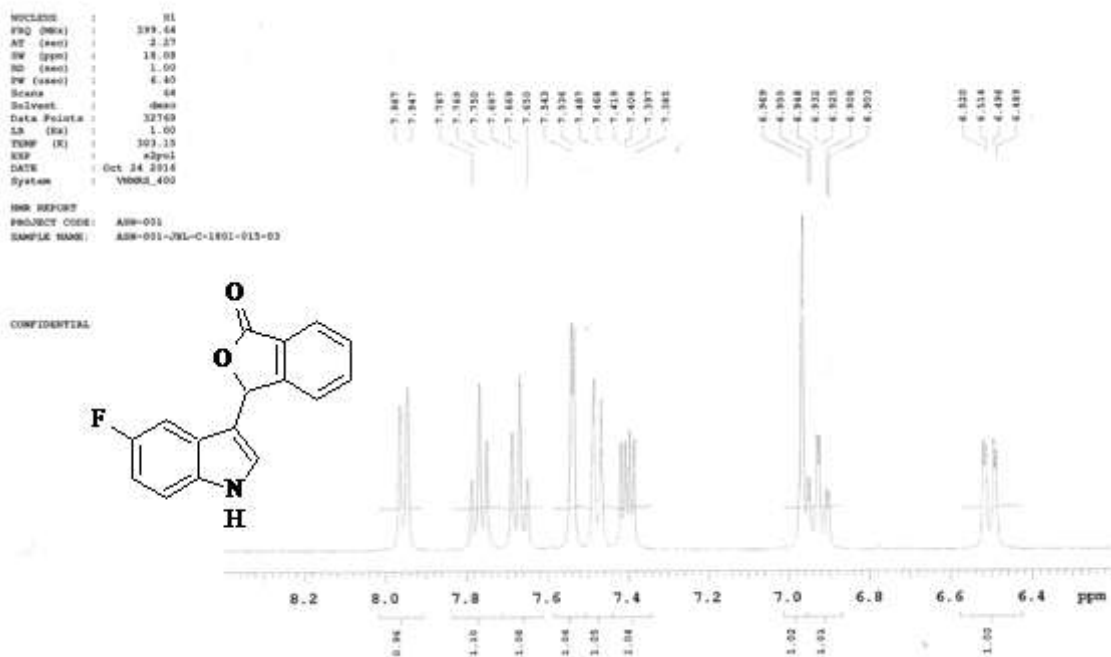
Figure 1(b): <sup>1</sup>H NMR Spectrum of 3-(1H-indol-3-yl)-2-benzofuran-1(3H)-one (4a)

Figure 2: IR Spectrum of 3-(1H-indol-3-yl)-2-benzofuran-1(3H)-one (4a)

Figure 3(a):<sup>1</sup>H NMR Spectrum of 3-(5-fluoro-1H-indol-3-yl)-2-benzofuran-1(3H)-one (4b)Figure 3(b):<sup>1</sup>H NMR Spectrum of 3-(5-fluoro-1H-indol-3-yl)-2-benzofuran-1(3H)-one (4b).



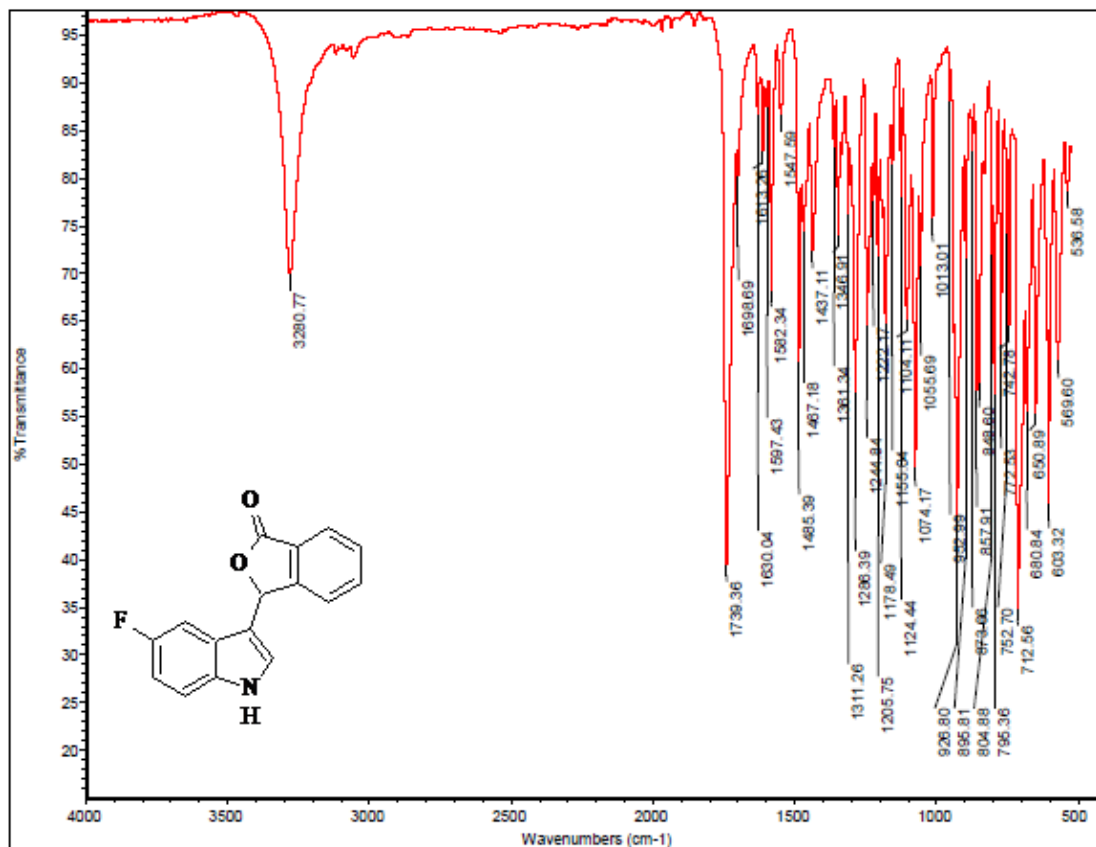


Figure 4: IR Spectrum of 3-(5-fluoro-1H-indol-3-yl)-2-benzofuran-1(3H)-one (4b).

#### Spectral data of 3-(1H-indol-3-yl)-2-benzofuran-1(3H)-one (4a)

IR (KBr) ( $\nu_{\max}/\text{cm}^{-1}$ ): 3311 (N-H), 3055 (C-H), 1732 (C=O), 1615 (C-C), 1287 (C-N), 1073(=C-H). <sup>1</sup>H NMR (400 MHz, DMSO):  $\delta$ =6.786 (d,  $J$  = 8.00 Hz, 1H), 6.874 (t,  $J$ =7.00 Hz, 1H), 6.965 (s, 1H), 7.082 (t,  $J$ =7.6 Hz, 1H), 7.402 (d,  $J$ =8.4 Hz, 1H), 7.462 (d,  $J$ =7.2 1 H), 7.499(s, 1H). 7.672 (t,  $J$ =7.6 Hz, 1H), 7.766 (t,  $J$ =7.6 Hz, 1H), 7.959 (d,  $J$ =7.60 Hz, 1H), 11.31 (s, 1H) ppm.

#### Spectral data of 3-(5-fluoro-1H-indol-3-yl)-2-benzofuran-1(3H)-one (4b)

IR (KBr) ( $\nu_{\max}/\text{cm}^{-1}$ ): 3280 (N-H), 3055 (C-H), 1739 (C=O), 1311 (C-N), 1074(=C-H). <sup>1</sup>H NMR (400 MHz, DMSO):  $\delta$ =6.520 (d,  $J$ =2.4 Hz, 1H), 6.955 (d,  $J$ =5.6 Hz, 1H), 6.969 (s, 1H). 7.397 (t,  $J$  = 4.8 Hz, 1H), 7.419 (d,  $J$ =4.4 Hz, 1H), 7.487(s, 1H), 7.669 (t,  $J$ =7.6 Hz, 1H), 7.787 (t,  $J$ =7.2 Hz, 1H), 7.967 (d,  $J$ =8 Hz, 1H), 11.441 (s, 1H) ppm.

#### Crystal structure analysis

The molecular structure of the title compound C<sub>16</sub>H<sub>10</sub>FNO<sub>2</sub> has been confirmed by single crystal X-ray diffraction analysis, which revealed that the compound crystallizes in the orthorhombic space group *Pbca* with unit cell parameters  $a = 16.5775(4)$  Å,  $b = 7.5072(2)$  Å,  $c = 20.1067(5)$  Å,  $\alpha = \beta = \gamma = 90.00^\circ$ ,  $Z = 8$ ,  $V = 2502.29(11)$  Å<sup>3</sup>. The ORTEP of the molecule with displacement ellipsoids drawn at 50 % probability level is shown in **Figure 5**. The crystal data and the structure refinement details are given in **Table 1**. The molecule is non-planar whereas both the fluoro-indole and the benzopyran rings are planar with the atoms C2 and C11 deviating 0.023(1) Å and 0.035(1) Å from their mean planes respectively. The dihedral angle between the two fused ring planes is 85.15(4)° indicating that they are nearly orthogonal to each other. The structure exhibits intermolecular hydrogen bonds of the type N—H...O and C—H...O. The hydrogen bond N1—H1...O20 has a length of 2.7921(16) Å and an angle of 153° whereas the other hydrogen bond C11—H11...O12 has a length of 3.3238(16) Å and an angle of 154° with symmetry codes  $-1/2+x,y,3/2-z$  and  $1-x,1/2+y,3/2-z$  respectively.

These hydrogen bonds links the molecules to chains and the molecules exhibit layered stacking when viewed down along the *b* axis (**Figure 6**).

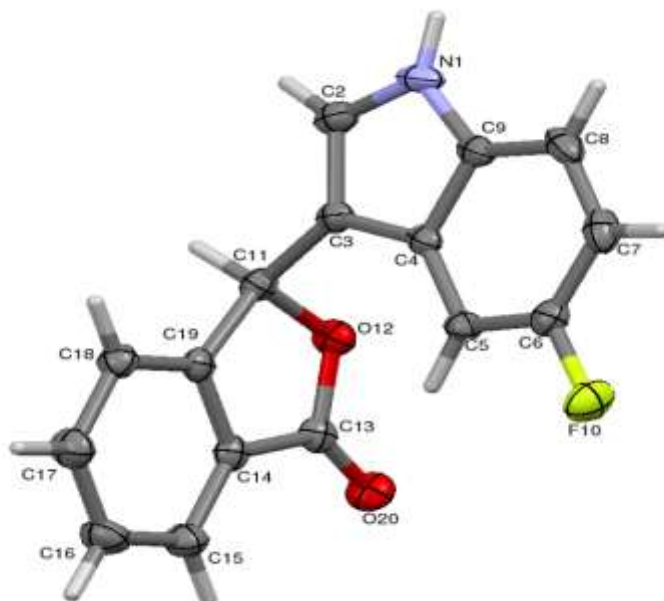


**Figure 5:** ORTEP of the molecule with thermal ellipsoids drawn at 50% probability.

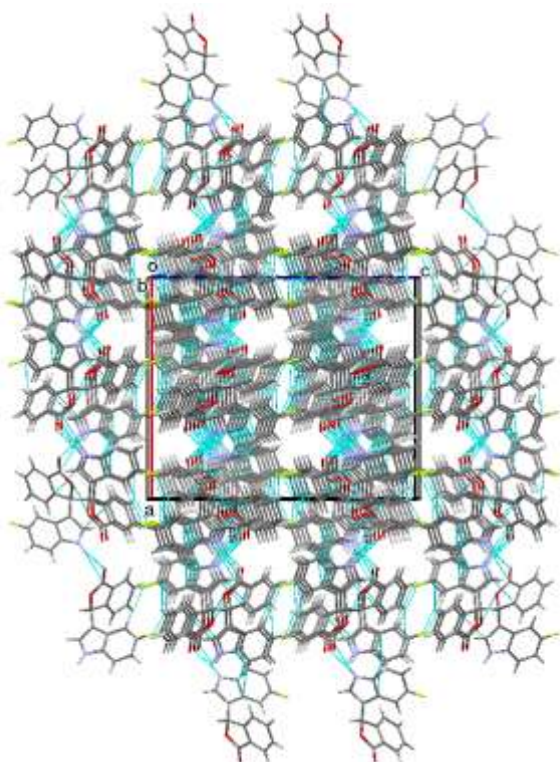


**Figure 6:** Packing of the molecules when viewed down along the *b* axis. The dotted line represents hydrogen bond interactions.

**Table 1:** Crystal data and structure refinement details

Parameter	value
CCDC deposit No.	CCDC 1511459
Empirical formula	C <sub>16</sub> H <sub>10</sub> FNO <sub>2</sub>
Formula weight	267.25



Temperature	296 (2) K
Wavelength	1.54178 Å
Crystal system, space group	Orthorhombic, <i>Pbca</i>
Unit cell dimensions	$a = 16.5775(4)$ Å $b = 7.5072(2)$ Å $c = 20.1067(5)$ Å $\alpha = \beta = \gamma = 90.00^\circ$
Volume	2502.29(11) Å <sup>3</sup>
Z	8
Density(calculated)	1.419 Mg m <sup>-3</sup>
Absorption coefficient	0.871 mm <sup>-1</sup>
$F_{000}$	1104
Crystal size	0.29 × 0.26 × 0.22 mm
$\theta$ range for data collection	4.40° to 64.71°
Index ranges	$-10 \leq h \leq 12$ $-6 \leq k \leq 8$ $-23 \leq l \leq 20$
Reflections collected	12616
Independent reflections	2068 [R int = 0.0335]
Absorption correction	multi-scan
Refinement method	Full matrix least-squares on $F^2$
Data / restraints / parameters	2068 / 0 / 181
Goodness-of-fit on $F^2$	1.122
Final [ $I > 2\sigma(I)$ ]	$RI = 0.0343$ , $wR2 = 0.0978$
R indices (all data)	$RI = 0.0354$ , $wR2 = 0.0989$
Largest diff. peak and hole	0.169 and $-0.210$ e Å <sup>-3</sup>

**Table 2: Bond lengths (Å)**

Atoms	Length	Atoms	Length
C4-C5	1.406(2)	C11-O12	1.485(2)
C4-C9	1.415(2)	C11-C19	1.505(2)
C4-C3	1.437(2)	O12-C13	1.357(2)
N1-C2	1.359(2)	C13-O20	1.212(2)
N1-C9	1.377(2)	C13-C14	1.465(2)
C2-C3	1.369(2)	C14-C19	1.382(2)
C3-C11	1.482(2)	C14-C15	1.386(2)
C5-C6	1.366(2)	C15-C16	1.381(2)
C6-F10	1.370(2)	C16-C17	1.395(2)
C6-C7	1.394(2)	C17-C18	1.388(2)
C7-C8	1.379(2)	C18-C19	1.388(2)
C8-C9	1.393(2)		

**Table 3: Bond angles (°)**

Atoms	Angles	Atoms	Angles
C5-C4-C9	119.02(13)	C3-C11-O12	109.91(11)
C5-C4-C3	134.31(12)	C3-C11-C19	117.06(11)
C9-C4-C3	106.64(12)	O12-C11-C19	102.85(10)
C2-N1-C9	109.22(11)	C13-O12-C11	110.74(10)
N1-C2-C3	110.32(13)	O20-C13-O12	121.51(12)

C2-C3-C4	106.41(12)	O20-C13-C14	129.71(13)
C2-C3-C11	125.53(13)	O12-C13-C14	108.78(11)
C4-C3-C11	128.03(12)	C19-C14-C15	122.50(13)
C6-C5-C4	116.92(13)	C19-C14-C13	108.34(12)
C5-C6-F10	118.10(13)	C15-C14-C13	129.16(12)
C5-C6-C7	124.59(14)	C16-C15-C14	117.04(13)
F10-C6-C7	117.31(12)	C15-C16-C17	120.96(14)
C8-C7-C6	119.18(14)	C18-C17-C16	121.56(14)
C7-C8-C9	117.93(13)	C19-C18-C17	117.43(13)
N1-C9-C8	130.21(13)	C14-C19-C18	120.50(13)
N1-C9-C4	107.41(12)	C14-C19-C11	109.23(11)
C8-C9-C4	122.35(13)	C18-C19-C11	130.25(12)

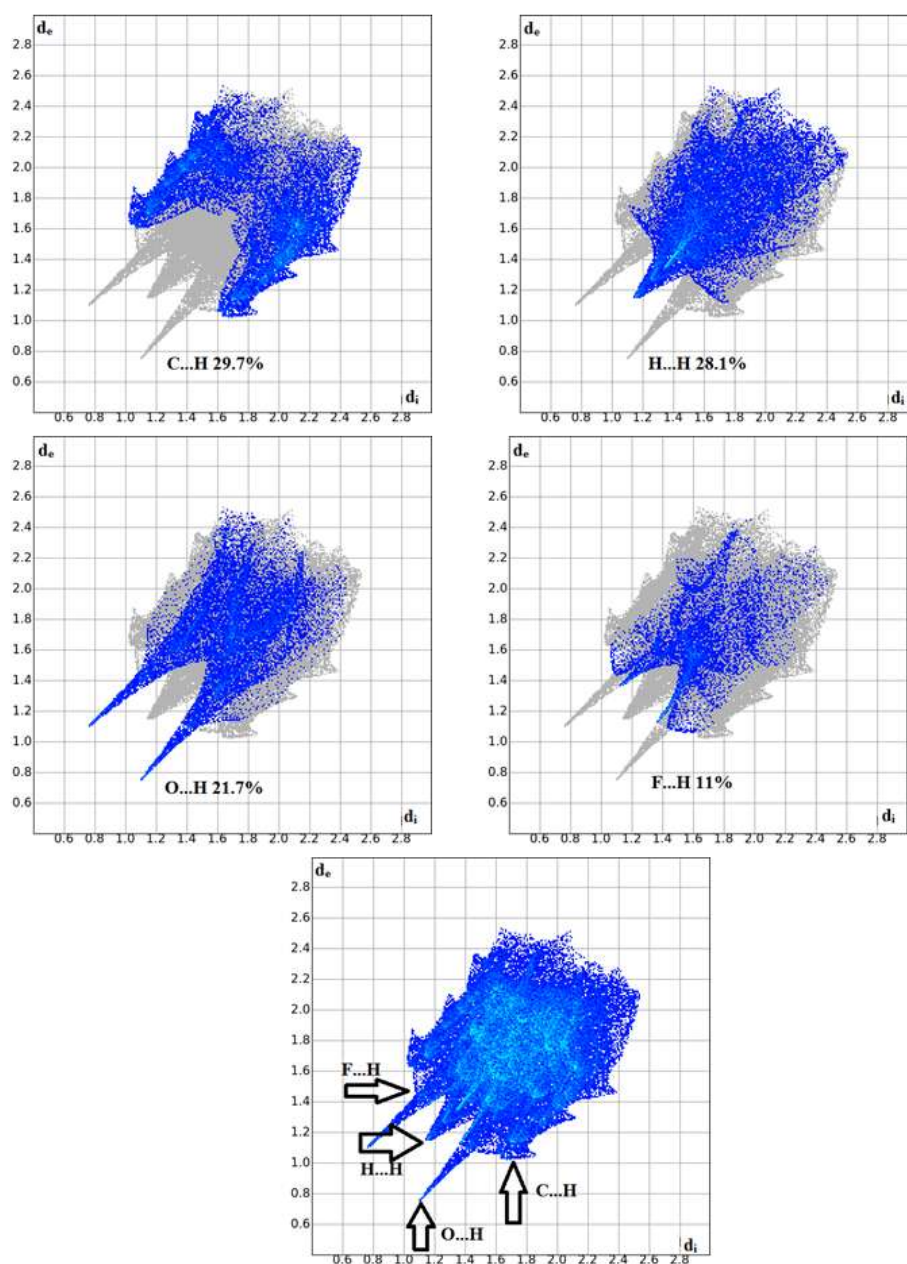


**Figure 7: Fingerprint plots of the title compound showing H...H, C...H, O...H and F...H interactions. Here  $d_i$  is the closest internal distance from a given point on the Hirshfeld surface and  $d_e$  is the closest external contacts.**

Hirshfeld surface analysis is an effective tool for exploring packing modes and intermolecular interactions in molecular crystals, as they provide a visual picture of intermolecular interactions and of molecular shapes in a crystalline environment. Surface features characteristic of different types of intermolecular interactions can be identified, and these features can be revealed by color coding distances from the surface to the nearest atom exterior ( $d_e$  plots) or interior ( $d_i$  plots) to the surface. This gives a visual picture of different types of interactions present and also reflects their relative contributions from molecule to molecule. Further, 2D fingerprint plots (FP), in particular the breakdown of FP into specific atom...atom contacts in a crystal, provide a quantitative idea of the types of intermolecular contacts experienced by molecules in the bulk and presents this information in a convenient colour plot. Hirshfeld surfaces comprising  $d_{norm}$  surface and Fingerprint plots were generated and analysed for the title compound in order to explore the packing modes and intermolecular interactions. The two dimensional fingerprint plots from Hirshfeld surface analyses **Figure 7**, illustrates the difference between the intermolecular interaction patterns and the relative contributions to the Hirshfeld surface (in percentage) for the major intermolecular contacts associated with the title compound. Importantly, C...H (29.7%) bonding appears to be a major contributor in the crystal packing, whereas the H...H (28.1%), O...H (21.7%), F...H(11%) plots also reveal the information regarding the intermolecular hydrogen bonds thus supporting for N—H...O and C—H...O intermolecular interactions. This intermolecular contact is highlighted by conventional mapping of  $d_{norm}$  and electrostatic potential on molecular Hirshfeld surfaces as shown in **Figure 8**. The red spots over the surface indicate the intercontacts involved in hydrogen bond. The dark-red spots on the  $d_{norm}$  surface arise as a result of the short interatomic contacts, i.e., strong hydrogen bonds, while the other intermolecular interactions appear as light-red spots.

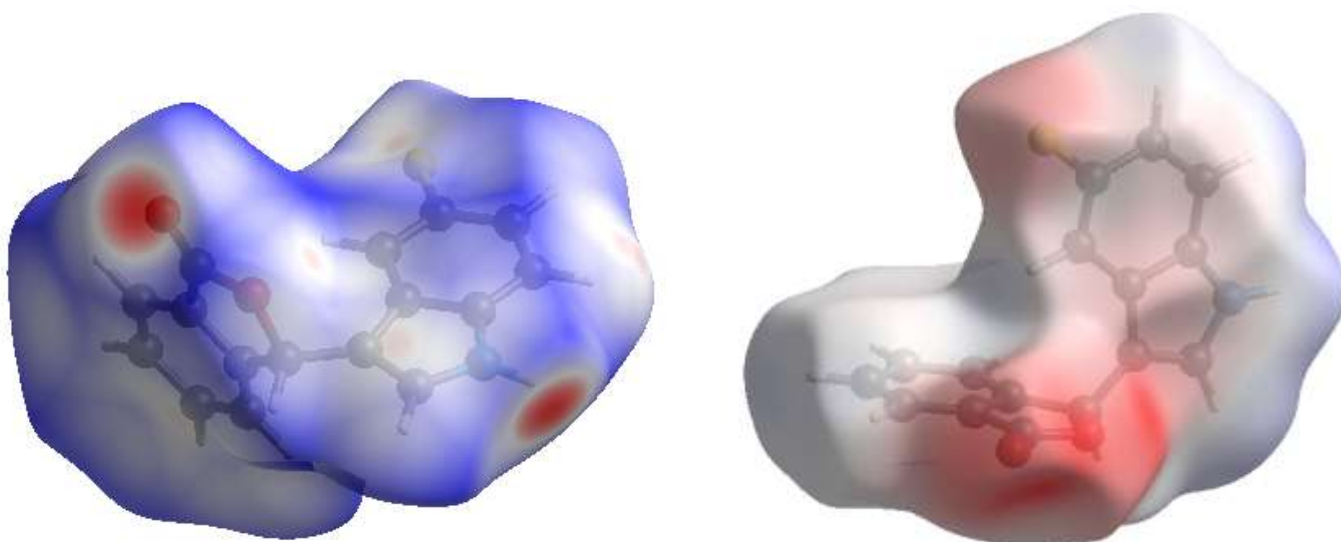


**Figure 8:**  $d_{norm}$  and electrostatic potential mapped on Hirshfeld surface for visualizing the intermolecular contacts

### Acknowledgements

The authors are thankful to the Institution of Excellence, VijnanaBhavana, University of Mysore, Manasagangotri, Mysore, for providing the single-crystal X-ray diffraction data. One of author R. Anil Kumar acknowledges to UGC New Delhi for financial support received from BSR fellowship.

### References

1. Sivosh M., Emerich S., Alfred P., Andreas S., SigurdE., Ute M., 3-Bromo-4-(1*H*-3-indolyl)-2,5-dihydro-1*H*-2,5-pyrroledione derivatives as new lead compounds for antibacterially active substances, *Eur. J. Med. Chem.*, 2006, 41,176-191.

2. Sivosh M., Emerich S., Alfred P., Andreas S., Sigurd E., Ute M., Antibacterial activity of a novel series of 3-bromo-4-(1*H*-3-indolyl)-2,5-dihydro-1*H*-2,5-pyrroledione derivatives – An extended structure–activity relationship study, *Eur. J. Med. Chem.*, 2008, 43, 633-656.
3. Prem P. Y., Prasoon G. A. K. C., Shukla P. K., Rakesh M., Synthesis of 4-hydroxy-1-methylindole and benzo[b]thiophen-4-ol based unnatural flavonoids as new class of antimicrobial agents, *Bioorg. Med. Chem.*, 2005, 13 1497-1505.
4. Wei-Jun Li, Xu-Feng Lin, Jun Wang, Guo-Liang Li, Yan-Guang Wang, A Mild and Efficient Synthesis of bis-Indolylmethanes Catalyzed by Sulfamic Acid, *Synth. Comm.*, 2005, 35, 2765–2769.
5. Bell R., Carmeli S., SarN., Vibrindole A., A Metabolite of the Marine Bacterium, *Vibrio parahaemolyticus*, Isolated from the Toxic Mucus of the Boxfish *Ostracion cubicus*, *J. Nat. Prod.*, 1994, 57, 1587–1590.
6. Carrillo G. P., Estrada J. G. G., Ramírez J. L. G., Toledano C. A., Infrared-assisted eco-friendly selective synthesis of diindolylmethanes, *Green Chem.*, 2003, 5, 337–339.
7. Safe S., Papineni S., Chintharlapalli S., Cancer chemotherapy with indole-3-carbinol, bis(3'-indolyl)methane and synthetic analogs, *Cancer Lett.*, 2008, 269, 326–338.
8. Shrunghesh Kumar T. O., Naveen S., Kumara M. N., Mahadevan K. M., Lokanath N. K., Synthesis, Characterization and Crystal structure Studies of 2-[(4-chlorophenyl)(1*H*-indol-3-yl)methyl]-1*H*-indole, *Acta Cryst.*, 2015, E71, o121.
9. Pradeep P. S., Naveen S., Kumara M. N., Mahadevan K. M., Lokanath N. K., Crystal structure of cis-1-(2-methyl-1, 2, 3, 4-tetrahydroquinolin-4-yl) azepan-2-one, *Acta Cryst.*, 2014, E70, o981-o982.
10. Pradeep P. S., Naveen S., Kumara M. N., Mahadevan K. M., Lokanath N. K., Crystal structure of 1-[(2*S*\*,4*R*\*)-6-fluoro-2-methyl-1,2,3,4-tetrahydroquinolin-4-yl]pyrrolidin-2-one, *Acta Cryst. Res. Comm.*, 2014, E70, 153-156.
11. Vindu Vahini, M., Devarajegowda H. C., Mahadevan K. M., Meenakshi T. G., Arunkashi H. K., Ethyl 3-oxo-3*H*-benzo[*f*]chromene-2-carboxylate, *Acta Cryst. E*66(2010) o2658.
12. Bruker, APEX, SAINT PLUS, Bruker AXS Inc., Madison, Wisconsin, USA, 2004;(b) Sheldrick G. M., *Acta Cryst.*, 1990, A46, 467.
13. Sheldrick G. M., Crystal structure refinement with SHELXL, *Acta Cryst.*, 2015, C71(1), 3-8.
14. Spek A. L., PLATON, an integrated tool for the analysis of the results of a single Crystal Structure Determination, *Acta Cryst.*, 1990, 46, c34-c34.
15. Macrae C. F., Bruno I. J., Chisholm J. A., Edgington P. R., McCabe P., Pidcock E., Rodriguez L. M., Taylor R., van de Streek J., Wood P. A., Mercury CSD 2.0-new features for the visualization and investigation of crystal structures, *J. Appl. Cryst.*, 2008, 41, 466-470.
16. Wolff S. K., Grimwood D. J., McKinnon J. J., Turner M. J., Jayatilaka D., Spackman, M. A., *Crystal Explorer (Version 3.0)*, *University of Western Australia*, (2012).
17. Saikat Kumar Seth, Tuning the formation of MOFs by pH influence: X-ray structural variations and Hirshfeld surface analyses of with cadmium chloride, *Cryst. Engg. Comm.*, 2013, 15, 1772-1781.
18. Saikat Kumar Seth, Structural elucidation and contribution of intermolecular interactions in O-hydroxy acyl aromatics: Insights from X-ray and Hirshfeld surface analysis, *J. Mol. Struct.*, 2014, 1064, 70-75.

\*\*\*\*\*